Transactions of the **14th International Conference on Structural Mechanics in Reactor Technology** (SMiRT 14), Lyon, France, August 17-22, 1997

L05/1

Creep damage and creep crack initiation under mode II loading in 316L steel. Experimental data and modelling

Poquillon D.[(1)], **Cabrillat M.T.**[(1)], **Pineau A.**[(2)]
(1) CEA, France
(2) URA CNRS 866, France

ABSTRACT
This study deals with the evaluation of the local approach applied to creep crack initiation. The first part of the paper describes original creep experiment with sharply notched thin wall tubular tested specimens in torsion, while the second part is concerned with the numerical modeling of creep damage and creep crack initiation. The chosen damage model was identified previously and is based on quantitative observations of grain boundary damage. This model is used in a finite element code in order to simulate creep crack initiation. Different constitutive equations are tested and calculated damage fields at the crack tip are compared with the observed experimental damage.

INTRODUCTION.
A number of components of fast breeder reactors operate at elevated temperatures, within the the creep range. At these temperatures, damage in 316 LN austenitic stainless steel cracked bodies which takes place during dwell period is mainly intergranular.

Many experiments were carried out under Mode I loading, when the load is applied normal to the crack plane. In a former study [1], it was shown that even under pure Mode I loading the directional aspect of creep crack initiation was dependent on other parameters than K_I but also on stress triaxiality ratio. A number of studies (see e.g. [2,3]) carried out on notched specimens have also shown that creep intergranular damage was dependent on stress triaxiality. However to the knowledge of the authors, the results of pure in-plane shear creep tests (Mode II) have never been reported. Therefore, in order to get a better understanding of the stress triaxiality effect on creep damage ahead of a crack tip, Mode II creep test with sharply notched thin wall tubular specimens in torsion was performed in the present study.

In the first part of this paper, we describe such a test in which the metallurgical observations of the sample revealed severe intergranular damage and crack initiation. In these observations a special emphasis was laid on the localization of intergranular damage.

The second part of the study is devoted to the modeling of creep crack initiation. A creep damage model is chosen, and introduced in a finite element code. Various constitutive equations are tested and calculated damage fields at the crack tip are compared with the experimental observations.

EXPERIMENTAL RESULTS

Specimen geometry.
The test sample is a sharply notched thin wall tubular specimen made in austenitic stainless steel 316 LN SPH (SQ heat).

The detailed composition of this material can be fund in [4], and it is given in Table 1.

The internal radius of the tubular specimen is 8.25 mm, while the wall thickness is 1.5 mm. A sharp EDM notch was made through the thin wall of the tube on 14.2% of the circumference (initial notch length 2a=8.05 mm at mid thickness). The crack tip radius ρ is 0.1mm. The gauge length of the specimen is 35 mm.

	C	S	P	Si	Mn	Ni	Cr	Mo	N	B	Co	Cu	Ti	Nb	Al	Ta	Ca ppm
316 L SPH	< 0.03	< 0.025	< 0.035	< 0.5	1.6 à 2.0	12 à 12.5	17 à 18	2.3 à 2.7	0.06 à 0.08	< 0.0025	< 0.25	< 1.	-	-	-	< 0.15	-
SQ	0.028	0.001	0.028	0.3	1.88	12.46	17.31	2.44	0.075	0.0010	0.014	0.175	-	-	-	-	-

Table 1: Chemical specifications of 316 L SPH steel and SQ Heat chemical composition.

The load controlled creep test was carried out at 600°C during 600 hours.

The geometry and the loading conditions are summed up in Figure 1. The load is applied and controlled by an servo hydraulic tension-torsion machine.

Creep crack initiation and creep crack growth are detected with an electrical potential drop technique. In this study devoted to crack initiation, no calibration curve is used : the final crack advance measured after the test on the sample will be compared with the electrical potential drop curve. An angular displacement transducer is set on the tube, with a measurement basis of 10mm (cf. Figure 1).

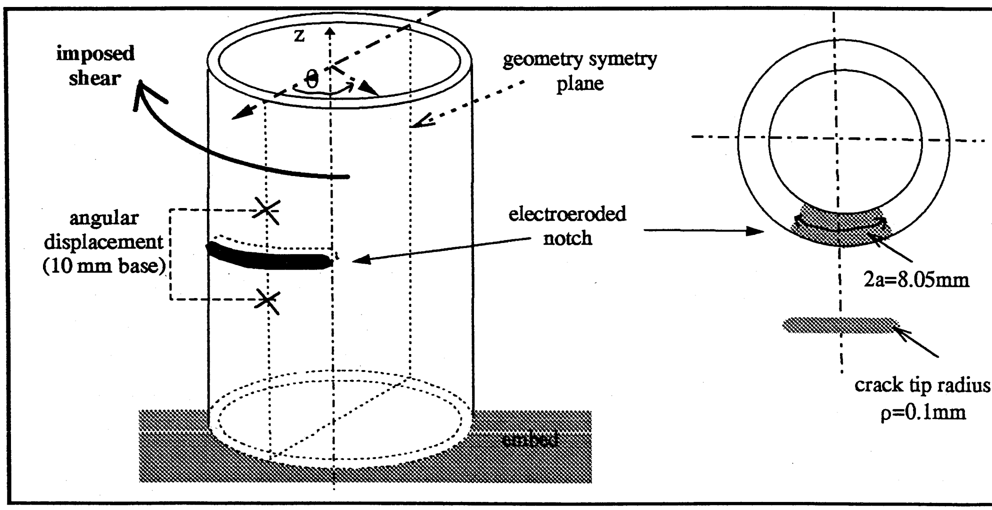

Figure 1 : Geometry and loading conditions of the specimen.

Test history, potential drop recording, angular displacement recording.

A torsional torque was imposed on the upper face of the tube and supposed to be constant through the thickness. The stress state on that upper face was thus pure shear. The tensile stress along the specimen axis was controlled and equal to zero. So we had $\sigma = \sigma_{\theta z} = 83$ MPa on the upper face of the tube.

The creep test had a 24 day duration. Aside a small perturbation after three days of test, the load was maintained constant all along the test. The variation of the torsional angle with time is shown in Figure 2 while the variations of the potential drop are reported on Figure 3.

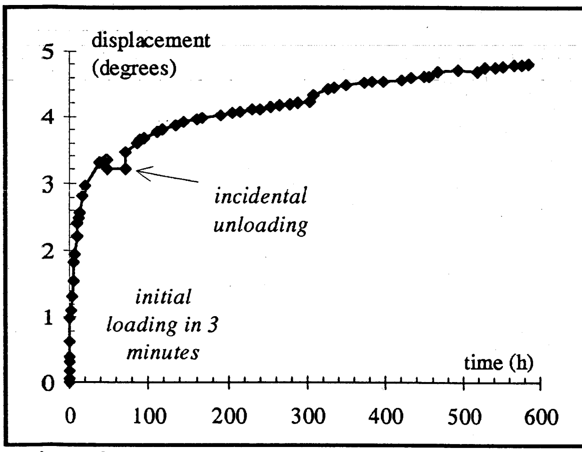

Figure 2 : Experimental angular displacement during Mode II creep test.

After about 13 days, the potential drop signal shows an average increase (Figure 3). We indicate on this curve the scattered band of the signal. Then a tendency curve can be obtained and crack initiation can be determined. This value of 13 days (about 320 hours) is correlated with an acceleration of the angular displacement observed exactly at the same time (Figure 2).

These two elements confirm a significant modification of the length of the sharp notch taking place 320 hours after the beginning of the creep test.

Microscopical observations.

The creep test was interrupted after 24 days. The tube was cut in order to measure both the internal and the external crack length. These measurements showed that a crack was initiated from the initial sharp notch and that the crack growth increments were the following :

- Inner wall final crack length increment : 2Δa=0.71 mm
- Outer wall final crack length increment: 2Δa=0.89 mm

The average crack growth in the initial notch direction is therefore Δa=400 µm (at each notch tip).

Metallurgical observations were made after careful polishing and chemical etching to reveal grain boundaries.

These observations showed that the fracture is intergranular (Figures 4 and 5). If the initial sharp notch (observations were made at 4 crack tips : 2 on the inner wall and 2 on the outer wall of the tubular specimen) propagates in its initial plane, important crack branching on the tension faces was noticed. Furthermore, many secondary intergranular cracks were observed

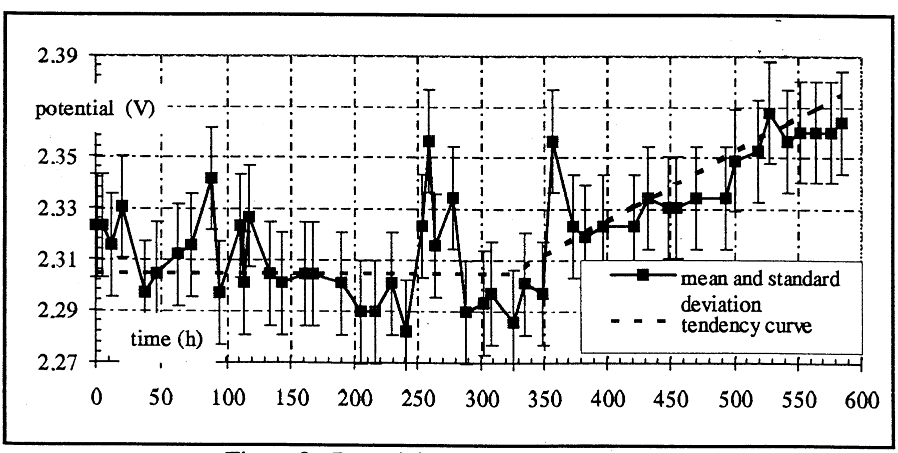

Figure 3 : Potential drop signal versus time.

far behind the tip of the initial sharp notch in a direction nearly perpendicular to the crack axis,

Figure 4 : An outer wall notch tip with cracks

on the tension surface of the EDM notch

Furthermore, in a large zone around the crack tip, many grain boundaries were broken along a 50-60° direction with the crack plane (i.e. Figure 5).

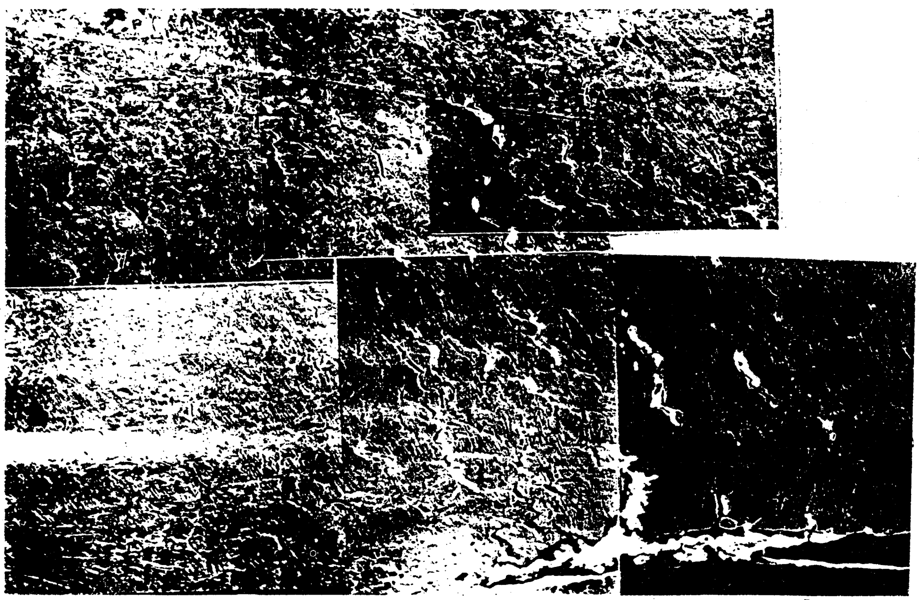

Figure 5 : Inner wall crack tip with a large zone where many grain boundaries are broken in a 50-60° direction with the crack plane. The white spots are due to the polymer which was applied on the surfaces to protect the relief (cracked grain boundaries).

In figure 6, taken close to the crack tip, besides intergranular cavities, intense slip bands are noticeable. This indicates, as the other figures, that crack initiation and crack growth are associated with large plastic strains.

Figure 7 summarises the observations made on the inner wall of the tube. No qualitative difference were noticed between the inner and the outer wall but the propagation is slightly more important on the last one ($2\Delta a$=890 µm instead of 710 µm).

To conclude about this test, four main points appear.

- Intergranular crack initiation and crack growth take place at the tip at a sharply EDM notch submitted to pure shear at 600°C.
- Crack branching is important, but the main cracks are between θ=0 at θ=60° (θ>0 is the part of the tip in tension).
- The damage zone, where cracked grain boundaries are observed, has a large extension at the crack tip.
- Damage was never observed in compressive zone.

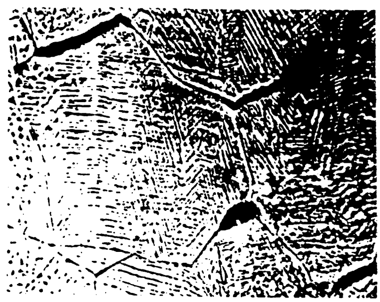

Figure 6 : Zoom at one of the inner wall crack tip on the cracked grain boundaries and intense slip bands

FINITE ELEMENT MODELING.

Constitutive equations.

Two different models were compared. The first one is isotropic elastoplasticity followed by combined creep (primary and secondary creep). The second one is the Chaboche viscoplastic model.

Model n°1: We used the material constitutive model taken from [4]. Two different mechanical models are combined : elastoplasticity (elastoplastic isotropic behaviour with the true stress-strain curve in uniaxial tension) during the initial loading followed by creep under steady load. The creep behaviour is a combination of primary and secondary creep. Both creep laws are isotropic. Primary creep is assumed to follow strain hardening rule

Model n°2: We used the Chaboche viscoplastic model [5]. This model is used in a two centre kinematics and isotropic form. The 24 coefficients of the model were taken from [6]. Some minor changes were made for a better fit with the SQ heat properties.

As this model has a single inelastic strain, the creep strain is assumed to be the strain occurring during hold time whereas the plastic strain is assumed to occur during the initial loading. So we introduced a new scalar field : the effective creep strain, which is the effective Mises inelastic strain occurring during hold time.

Intergranular damage law.

A number of metallurgical studies [7-17] devoted to stainless austenitic steel damage at high temperature generally agree with the following characteristics of this damage :

- it is perpendicular to the principal stress,
- it is sensitive to inelastic strain,
- and to the effective Mises stress,
- it occurs only in tensile hold time.

But the damage criterion and fracture criterion used in modeling the phenomenon depend on authors. And the real difficulty of the problem comes from the gap between the two points of view : the void-scale (μm) and the engineer-scale.

We used the local approach to fracture to predict crack initiation. The chosen creep damage law is not coupled with the viscoplastic behaviour : mechanical fields are used to compute the damage but the damage does not modify the mechanical stress-strain fields.

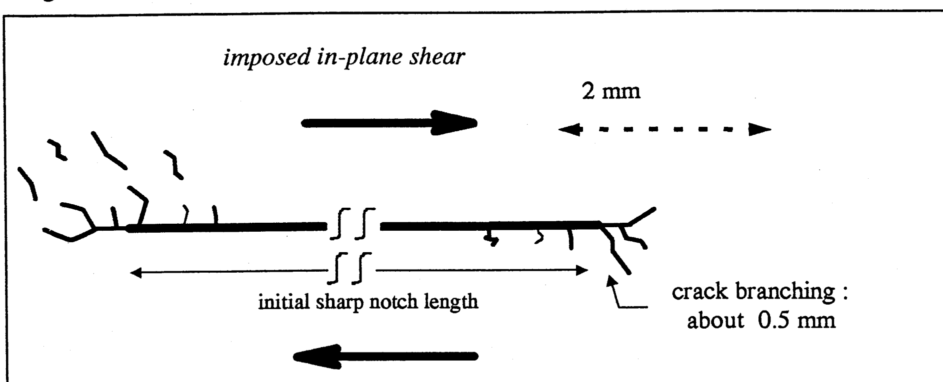

Figure 7: Scheme of the intergranular cracks on the inner wall of the tube.

This damage law is based on detailed metallographical observations made on a materiel similar to the steel used in the present study [2-4, 7]. In these studies, it was shown that the intergranular damage (a damage scalar field D) can be expressed as :

$$dD = A\langle\sigma_1\rangle^2 \frac{1}{\sqrt{\varepsilon_{e\_cr}}} d\varepsilon_{e\_cr} \tag{1}$$

where $\langle x \rangle = x$ if $x>0$, $\langle x \rangle = 0$ if $x<0$, A is a constant (2 10^{-5}), σ_1 is the maximum principal stress (MPa) and ε_{e_cr} the effective Mises creep strain.

In Eq. 1, the incremental damage is integrated along the stress-strain path. It is assumed that the fracture criterion is D=Dc with Dc=2.5.

We have chosen this model because it was firmly qualified from numerous tests on notched specimens [1, 4, 18]

Meshes and limit conditions.

Two different F.E. simulations were made : a simplified 2D one and a complete 3D one.

2 D simulation of a representative notched plate submitted to in-plane shear creep test.

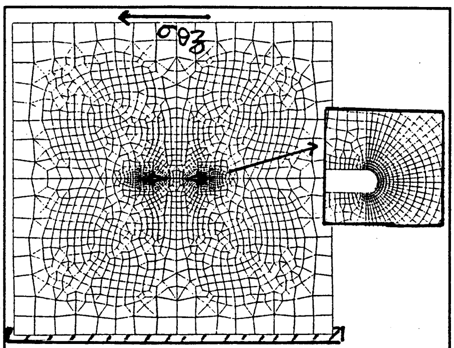

Figure 8 : 2D mesh of a notched plate in plane stress submitted to in-plane shear.

The mesh was supposed to represent the 'unrolled 'tube and so the ratio between the notch length and the width of the plate was 14.2%.

Because of the small thickness of the sample, this simplified model was a 2D notched plate in plane stress submitted to in-plane shear stress $\sigma_{\theta z}$ as detailed on the mesh of Figure 8. The mesh size at the tip of the notch is of 10µm.

Of course, this simplified modeling was enable to give us inner/outer wall effect as well as axisymmetrical 3D effects. But this simulation was done before the test to design the shear stress to be imposed in order to get a significant damage at the notch tip in some hundreds hours.

To sum up, the purpose of this mesh was to follow the time evolution of the maximum of damage at the notch tip but not to give us realistic data about its localization.

3 D simulation of in-plane shear creep test of a sharply notched thin wall tubular specimens in torsion.

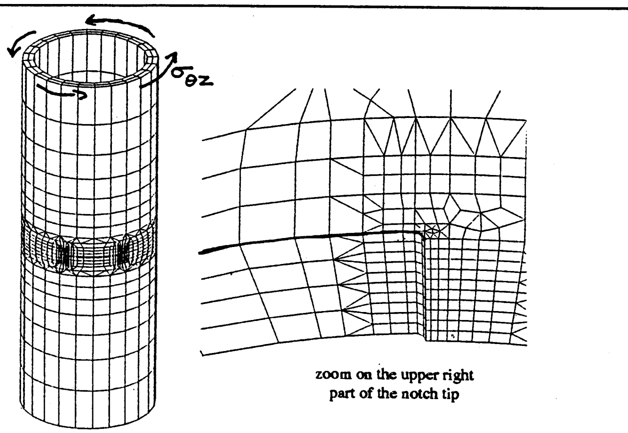

Figure 9 : 3D mesh of the thin wall tubular specimen in torsion and loading conditions.

Figure 9 shows the mesh used to simulate the test with more accuracy. It is a 5230 node 3D mesh.

At the notch tip, the thickness is divided in 10 elements, in order to see the difference between the inner and the outer wall part of the notch.

The lower part of the sample is fixed (all the displacements are blocked, cf. Figure 1), and a stress field is imposed on the upper face ($\sigma = \sigma_{\theta z} = 83$ MPa).

F.E. CALCULATIONS RESULTS.

The finite element code used is Castem 2000 [19]. It can cope with parametrical mesh, inelastic behaviour (plasticity, viscoplasticity...) large displacements option and fundamental operations on tensors (damage field computation).

2 D simulation.

This simulation was based on model n°1 with a 83 MPa shear stress. Damage is observed to be maximum at about 60° from the sharp notch plane, along the face which is under tensile

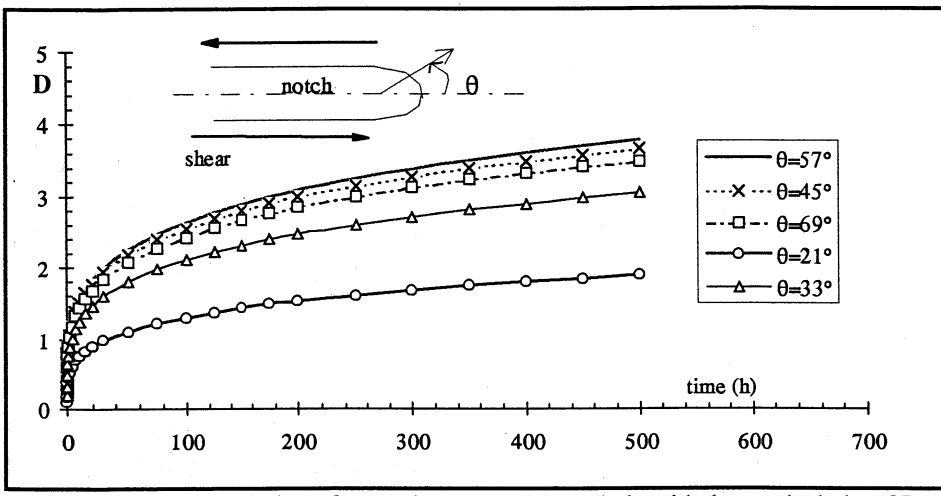

Figure 10 : Time evolution of creep damage at the notch tip with the notched plate 2D simulation.

loading. The time evolution of creep damage is given on Figure 10 and the critical value Dc=2.5 is reached after about 100 hours at the very notch tip. After 500 more hours, damage zone extends beyond 50 µm.

On the one hand this value was short enough to show the feasibility of the test, on the other hand, it was long enough to let significant creep strain developed in the sample. Other shear stress values were tested. The 83 MPa value is a compromise to have significant creep strain and damage and to limit the buckling risk of the specimen.

3 D simulations.

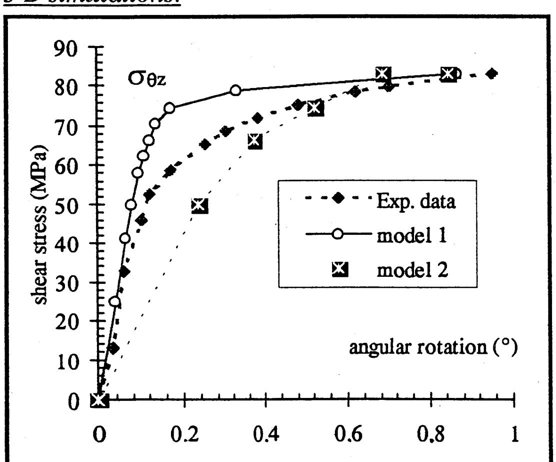

Figure 11 : 3D simulations of the initial loading angular displacement

On that more sophisticated mesh, both models n°1 and n°2 were used.

Initial loading.

The comparison between experimental angular displacement and the numerical simulations is satisfactory (Figure 11). Model 1 and model 2 are in good agreement with experimental data but tend to slightly underestimate the displacement angle at the end of the initial loading. As the constitutive equations were established from tensile tests, some little difference with shear tests are not very surprising.

Creep behaviour.
Both model 1 and model 2 underestimate the angular displacement during the first ten hours of creep. But at the end of the 600 hour creep test, model 2 gives a displacement rate in good agreement with experimental data whereas model 1 largely underestimates the creep strain rate (Figure 12).

The difficulty of behaviour modeling comes here from at least two points :

- The lack of data comparing shear test and tension test.
- The impossibility to have a perfect creep model in a wild range of stress. In our case creep law identification were done between 150 MPa and 300MPa. And to be realistic at the crack tip (so at the upper part of the range) leads to an underestimation of the creep rate at the lower part of the range ($\sigma_{\theta z}$=83 MPa implied σ_{eq} =144MPa).

As the purpose of this study is the damage field at the crack tips, we wouldn't focus more on the global displacement curves. Both behaviour models are more relevant at higher stress level.

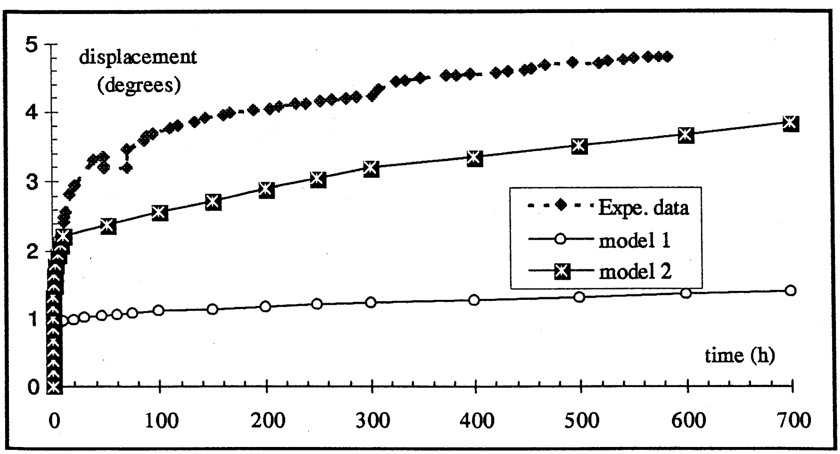

Figure 12 : 3D simulation of the creep, angular displacement.

Damage and mechanical fields at the crack tip.
During creep, as at the end of the loading, mechanical fields at the notch tip derived from both models are nearly similar. But as model 2 gives angular displacement in better agreement with the experimental data, we will essentially comment results obtained with this constitutive equation.

The results of damage computations can be summarized as following :

1. After an important development during the first fifty hour, intergranular damage growth occurs continuously (same qualitative development as for the 2D simulation on Figure 10).
2. An important creep damage develops behind the tip of the notches (Figure 13).
3. Damage develops slightly more on the outer wall than on the inner wall (Figure 13).

4. The mechanical fields differ in their shape between the outer wall and the inner wall : the outer wall presents isovalue curves with more circumferencial extension, whereas the inner wall presents isovalue curves with a noticeable extension in the z direction too. This remark applies to the equivalent creep strain as well as to the maximum principal stress and, as a consequence, to the damage.
5. After 600h of creep the zone were D is larger than to Dc=2.5% corresponds to a 300-350 μm zone located in front of the crack tip (Figure 13).

Comparison with experimental observations.

- Point 1 is difficult to compare with any experimental result, as damage growth is impossible to connect with the potential drop curve. We can just be sure that after 300 hours of creep loading, the damage zone where D>Dc as a size of about 200-300 μm. The size of the mesh at the crack tip is not small enough to have a better precision.
- Point 2 is in good agreement with cracked grain boundaries observed for example on Figures 4 and 5 behind the notch and far from the notch tip 400-500 μm. These secondary cracks were always short (about 100μm). The damage is there localised near the surface of the notch.
- Points 3 and 4 remind us that the experimental measurements of crack growth had shown that the two outer wall cracks were longer than the two inner wall cracks. The 3D damage computations account for this observation.
- Point 5 shows that the experimental length of crack propagation in the direction of the initial notch corresponds to the size of the calculated zone were D is larger than Dc=2.5.

The large zone around the crack tip, where many grain boundaries of the specimen are cracked in a 50-60° direction (see Figure 5) does not correspond to the extension of the computed damage field. This difference might arise either from the coldworking associated with the machining of the EDM notch or to the mechanical rigidity of 8 node cubic elements used in the mesh at the tip of the notch.

It is clear that further tests must be performed to confirm the tendencies observed in the present study. These tests are currently underway.

To conclude on these F.E. simulations, we would like to point out again the general good agreement with the experimental data about :

- the differences between inner and outer wall cracks (3D mesh),
- the damage zone behind the notch tip, on the surface in tension where secondary cracks develop perpendicular to the EDM notch,
- the dominant damage zone in front on the notch tip, from the initial axis to 60° on the side in tension, where the longest intergranular cracks are initiated,
- the sizes of these zones after 600h of creep.

We will insist on the fact that the constitutive equation and damage model used in the present study were identified on tensile tests, and no specific data were available about the material under shear loading. Further tests are necessary to check the representativity of these models when they are applied to torsional loading.

CONCLUSIONS.

In order to get a better understanding of stress triaxiality effect on creep damage ahead of a sharp notch, a first in-plane shear creep test was performed on a sharply notched thin wall

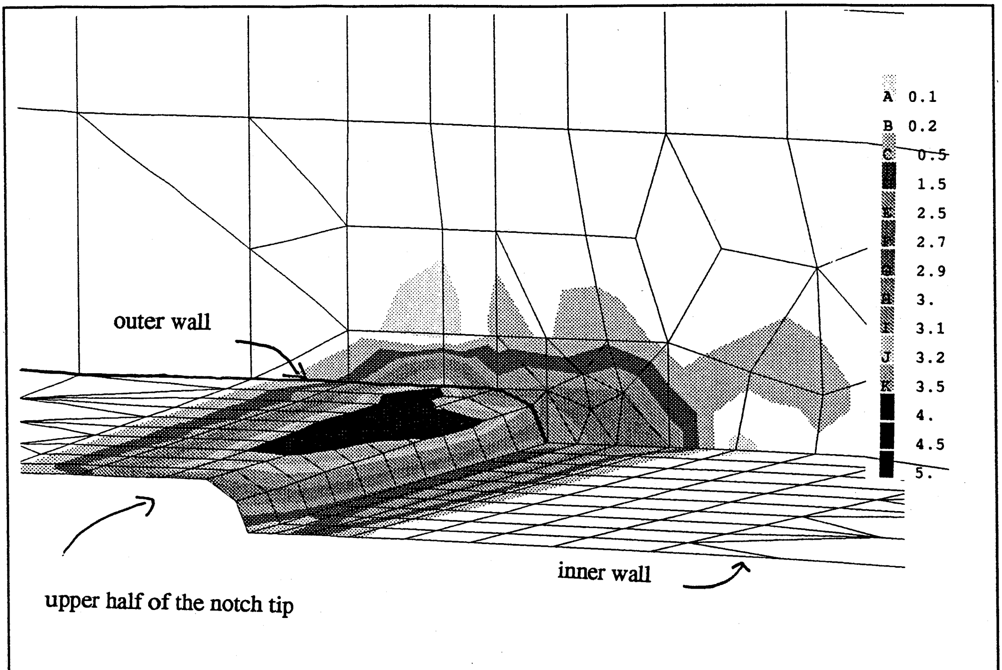

Figure 13 : Damage field at one of the notch tip after 600h.

tubular specimen tested under torsional loading. This test was performed at 600 °C during 600 hours and showed that a large amount of intergranular damage took place preferentially at the tip of the notches along the faces in tension. This intergranular damage produced crack initiation.

The comparison between metallurgical observations of cracked grain boundaries and 3D damage field computations shows the accuracy of the local approach to intergranular fracture, and confirms the validity of the incremental damage law applied to Mode II creep test. Further investigations are planed to confirm the accuracy of this damage law applied to stress triaxiality conditions.

REFERENCES.

1. Poquillon, D. 1996. Local approach : numerical simulation of creep crack initiation and growth. *NATO ASI, Mechanical Behaviour of Materials at High Temperature*; 217-225. Kluwer Academic Publishers ; Dordrecht.

2. Diboine, A. 1982. Influence de la triaxialité des contraintes sur la cavitation intergranulaire induite par fluage d'un acier austénitique. *D.E.A rapport, C.D.M, Ecole Nationale Supérieure des Mines de Paris.*

3. Yoshida, M. 1985. Endommagement intergranulaire de fluage dans un acier inoxydable 17Cr-12Ni : étude quantitative - rôle de la multiaxialité des contraintes. *Thesis, sciences et génie des matériaux, Ecole Nationale Supérieure des Mines de Paris.*

4. Piques, R. 1989. Mécanique et mécanismes de l'amorçage et de la propagation des fissures en viscoplasticité dans un acier inoxydable austénitique. *Thesis, sciences et génie des matériaux, Ecole Nationale Supérieure des Mines de Paris.*

5. Lemaitre, J. & J-L. Chaboche 1988. *Mécanique des Matériaux Solides.* Dunod, Paris.

6. Rive, D., C. Escaravage, B. Riou & M-T. Cabrillat 1991. Creep fatigue analysis of LMFBR'S structures. Identification of Chaboche's models for the stainless steel 316 SPH, *SMIRT 11, Tokyo*, paper L06/1.

7. Levaillant C. 1984. Approche métallographique de l'endommagement d'aciers inoxydables austénitiques sollicités en fatigue plastique ou en fluage. *Thesis; UTC Compiègne.*

8. Laiarinandrasana L. 1994. Amorçage et propagation de fissure à haute température dans un acier inoxydable austénitique. *Thesis, sciences et génie des matériaux., Ecole Nationale Supérieure des Mines de Paris.*

9. Hales R. 1994. The role of cavity growth mechanisms in determining creep-rupture under multiaxial stresses. *Fatigue Fract. Engng Mater. Struct, 17*, 5: 579-591.

10. Bestwick R.D. & D.E., Buckthorpe 1994. Strain based creep-fatigue design rules. *Fatigue Fract. Engng Mater. Struct 17*, 7: 849-859.

11. Ainsworth R.A. &P.J. Budden 1994. Design and assessment of components subjected to creep. *Journal of Strain Analysis, 29*, 3: 201-208.

12. Bensussan P., R. Piques R. & A. Pineau 1989. A critical assessment of global mechanical approaches to creep crack initiation and creep crack growth in 316L steel. *Non Linear Fracture Mechanics, vol I. Time Dependent Fracture, ASTM STP 995*: 27-54.

13. Skelton R. P. 1993. Damage factors during high temperature fatigue crack growth', *ESIS 15, Behaviour of defects at high temperatures.* Mechanical Engineering Publications, London: 191-217.

14. Riedel H. 1987. *Fracture at High Temperature*, Springer-Verlag; Berlin.

15. Saxena A. 1991 Creep crack growth in high temperature ductile materials. *Engineering Fracture Mechanics, 40*, 4/5: 721-736.

16. Bensussan P., E. Maas, R. Pelloux & A. Pineau 1988. Creep crack initiation and propagation : fracture mechanics and local approach. *Jour. of Pres. Vess. Technology , 110*: 42-50.

17. Maas E. & A. Pineau 1985. Creep crack growth behaviour of a 316L steel. *Engineering Fracture Mechanics 22, 2*: 307-325.

18. Poquillon D., M-T. Cabrillat & A. Pineau 1996. Local approach : numerical simulation of creep and creep-fatigue crack initiation and growth in 316 L SPH austenitic stainless steel. *Euromech-Mecamat'96 Proceedings. Local Approach to Fracture, Fontainebleau, France,9-11 sept. 96.*

19. Hoffmann A & A. Combescure 1978. Castem, a system of finite element computer programs. *Conference on Structural Analysis, Design and Construction in Nuclear Power Plant*, Porto Alegre, Brazil, paper 40.